Eur. Phys. J. B **17**, 595–601 (2000)

THE EUROPEAN PHYSICAL JOURNAL B

EDP Sciences

Correlation functions and the dynamical structure factor of quasicrystals

M. Hohl, J. Roth[a], and H.-R. Trebin

Institut für Theoretische und Angewandte Physik, Universität Stuttgart, Pfaffenwaldring 57, 70550 Stuttgart, Germany

Received 17 March 2000 and Received in final form 8 June 2000

Abstract. The icosahedral or decagonal symmetry of quasicrystals is well described by a periodic structure in higher dimensions. One consequence is the existence of dynamic phason modes in addition to the phonon modes. In an atomistic model phasons show up as correlated atomic jumps. We detect the phasons by the calculation of correlation functions and the dynamical structure factor in molecular dynamics simulations similar to the procedure used for phonons. In the simulations it is also possible to observe atomic jump processes directly. The models studied here represent icosahedral AlCuLi and decagonal AlCuCo quasicrystals. Ring processes are observed in the icosahedral case, and flips in the decagonal model.

PACS. 61.44.Br Quasicrystals – 66.30.-h Diffusion in solids – 68.45.Kg Dynamics; vibrations

1 Introduction

Quasicrystals possess dynamic phason modes in addition to the phonon modes. In an atomistic model phasons show up as correlated atomic jumps. Bak and Lubensky *et al.* [1,2] were the first to describe the properties of phasons in quasicrystals in a continuum model. The character of the phasons is diffusive in contrast to the propagating phonon modes.

Up to now, many experimental as well as theoretical investigations of the dynamical properties of quasicrystals have been concentrating on the phononic part of the dynamical spectrum.

Measurements of the phonon density in AlCuLi single crystals with inelastic neutron scattering by Goldman *et al.* [3] are in quantitative agreement with calculations by Hafner *et al.* [4] for low energy modes. De Boissieu *et al.* [5] and Boudard *et al.* [6] also have studied the phonon dispersion relation of i-AlPdMn single crystals with the help of inelastic neutron scattering. They observe isotropic acoustic modes. Band gaps which one expects due to quasiperiodicity have not been found. Longitudinal optical modes have been detected [6,7]. Suck has measured the generalized phononic density of states of d-$Al_{71}Pd_{19}Mn_{10}$ [7].

Hafner and his group have calculated in detail the dynamical structure factor of quasicrystals for the icosahedral Henley-Elser-type models [8] as well as for different decagonal models [9]. In their approach the dynamical matrix is used to compute the eigenvectors, eigenvalues, and participation ratios for each mode. The density of states and the dynamical structure factor were determined. In this approach the full interaction is replaced by a harmonic one and the strength of the springs enters the dynamical matrix. Jumps of the atoms, long-range diffusion and the nonlinearity of the interaction are neglected. Therefore the phasonic degrees of freedom of the quasicrystals are not taken into account. At low energies propagating modes exist with long wavelength and longitudinal and transversal acoustic character in icosahedral [4,10] and in decagonal [11] quasicrystals. The modes yield a linear and isotropic dispersion relation and lie in the vicinity of the strongest Bragg maxima (the Γ-point and its symmetry equivalent images). At higher energies a hierarchy of dispersionless optical modes around the points of high symmetry in the reciprocal lattice have been predicted and observed [7]. These points are equivalent to the pseudo-Brillouin zone boundaries. Some modes are localized at special positions of the quasilattice.

Further calculations with similar methods have been carried out by Los *et al.* [12] and by Kasner and Böttger [13] for simple quasicrystal models. The dynamical properties of AlMnSi quasicrystals have been investigated by Poussigue *et al.* [14]. The difference between the work of Hafner *et al.* and Poussigue *et al.* is that the latter observe the localization of the modes already for lower wave numbers and that it extends up to the pseudo-Brillouin zone boundaries.

Cockayne and Widom [15] have studied phason energetics in quasicrystals using realistic energetics but unphysical dynamics. Kalugin and Katz have conjectured that there exist new diffusion mechanisms in quasicrystals due to phasons [16]. A local rearrangement of the cells in a tiling model represents a process which leads to long-range diffusion (so called "flip" diffusion). The temperature

[a] e-mail: johannes@itap.physik.uni-stuttgart.de

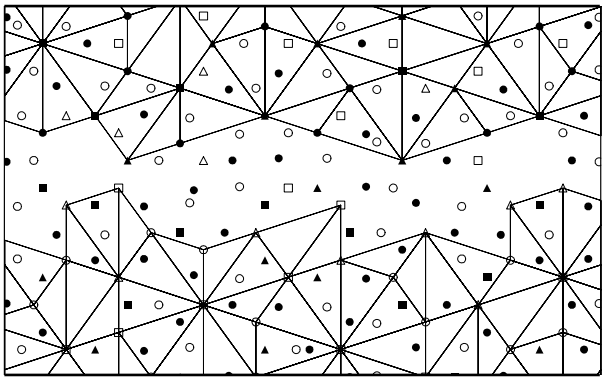

Fig. 1. Part of the d-AlCuCo model. In the upper region of the picture a part of the triangle tiling of layer one is shown and in the lower region a part of the triangle tiling of layer two. The symbols are: squares Co, triangles Cu and circles Al. Filled symbols are atoms in layer one and empty symbols in layer two.

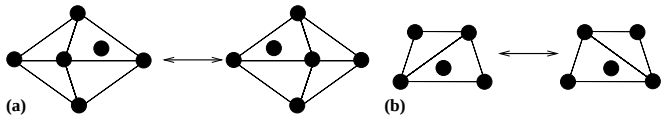

Fig. 2. (a) Simpleton flip (b) trapezoid flip.

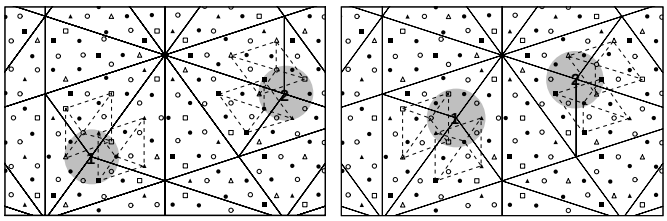

Fig. 3. Large tiling (full lines) from the Burkov decoration and some tiles of the triangle pattern which indicate the layers separately (broken lines). Left: initial configuration. Right: final configuration after two flips of the prismatic cluster. (From Ref. [25].)

dependence of the diffusion constant should deviate from an Arrhenius law [16]. The flip diffusion in tiling models has been recorded by several groups with Monte-Carlo simulations. As an example we cite reference [17].

Coddens *et al.* have observed jump processes in i-AlCuFe and i-AlPdMn directly by means of quasielastic neutron scattering and Mößbauer spectroscopy [18,19]. They show that the intensity of the quasielastic signal depends on temperature, but the width of the signal is independent, and they argue that this behavior contradicts the expectations of the Kalugin and Katz model [20]. The results can be interpreted as jumps of Cu and Pd to second-nearest neighbor places which implies a reordering of the clusters in the cluster model of the quasicrystals. It may also be possible that whole chains of atoms move. Angular dependent measurements show that the jumps occur preferably along twofold axis.

At least the observed activation energies and the prefactors of high temperature tracer diffusion experiments (see for example [21]) can be interpreted with high confidence as vacancy diffusion. New tracer diffusion experiments have extended the range of measurements down to 400 °C. At about 600 °C a new diffusion process overtakes the ordinary vacancy diffusion. Blüher *et al.* [22] speculate that this new process is flip assisted diffusion.

We have seen that up to now the dynamical properties of quasicrystals were studied mostly in the harmonic approximation. The characteristic properties have been obtained by diagonalizing a dynamical matrix. On the other hand the computation of the dynamical properties of liquids, glasses and crystals directly by molecular dynamics simulations has been carried out for years [23,24]. In this method the atoms are free to move under the influence of the forces which act on them. They also can change their sites. In the molecular dynamics approach one records the van-Hove correlation functions in space and time during a simulation and analyses them directly or one calculates the dynamical structure factor by a spatial Fourier transform (which yields the intermediate scattering function) and a Fourier transform in time. With the correlation functions it is possible to study diffusive and phasonic modes beyond the dynamical matrix approach.

The paper is organized as follows: First we describe the model quasicrystals and discuss geometric models for the phasonic flips (Sect. 2). A short discourse about the correlation functions (Sect. 3) and molecular dynamics (Sect. 4) follows. Then we present the results for AlCuCo and AlCuLi quasicrystals (Sect. 5).

2 The Models and jumps

2.1 The decagonal model

The starting point are flips which have been derived by Zeger for the Burkov model of AlCuCo [25,26]. In this work it has been demonstrated that each layer of AlCuCo quasicrystals may be represented with the help of triangle tilings (Fig. 1). In each layer the Co, Cu and a part of the Al atoms occupy the vertices of the particular triangle tiling, whereas the remaining Al atoms of the layer lie in the center of the acute-angled triangles. Since the possible flips in the triangle tiling are well-known, phasons may now be introduced into the AlCuCo model. If a simpleton flip is carried out two atoms move within a layer – they jump a distance of 0.87 Å – whereas in a trapezoid flip no atom moves (Fig. 2). Trapezoid flips are only required to change the tile arrangements determined by matching rules. Through a proper coupling of the simpleton flips between the layers one can describe the flip of tenfold prismatic clusters (Fig. 3), similar to the flips observed in experiment [27]. In the simulations we do not discern Co and Cu and thus make use of a binary Al-TM model.

2.2 The icosahedral model

The icosahedral model is a modification of the truncated icosahedral (TI) model described in [28]. In this model

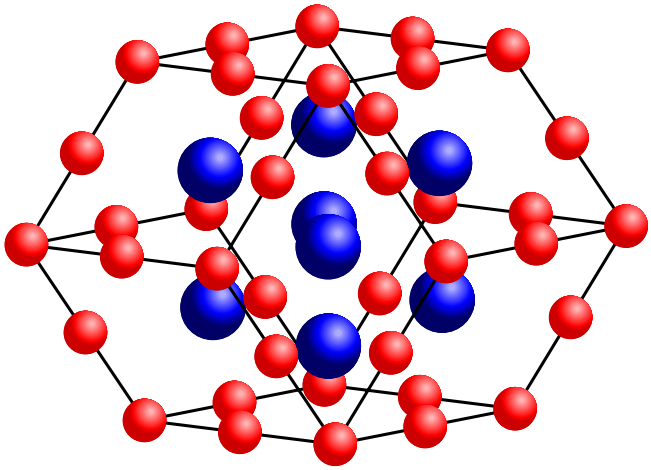

Fig. 4. The modified rhombic dodecahedron. The light atoms are small A atoms. The dark atoms in the interior are large B atoms.

the corners and the mid-edge points of the standard icosahedral rhombohedra are decorated with small A atoms representing Al or Cu. In the large prolate rhombohedron two additional large B atoms, representing Li are placed on the long cell diagonal dividing it in the ratio τ:1:τ, where τ is the golden mean. There are configurations where up to ten flat rhombohedra encircle a tiling edge. Atoms in this configuration may move around closed polygons with ten edges. These geometrically and energetically unstable configurations can be removed by the introduction of a further tile, the rhombic dodecahedron which replaces a pair of flat rhombohedra and a pair of large rhombohedra (Fig. 4). The dodecahedron is filled with a hexagonal bipyramid of B atoms. The model is called the Henley-Elser model or binary model [8]. Ring processes are effectively suppressed in this model. But the tiling flips, which take place in the dodecahedra of the TI model are also removed.

3 Correlation functions

The basis of our study is the evaluation of the van-Hove correlation function

$$G_{\mathrm{s}}(\mathbf{r},t) = \frac{1}{N}\left\langle \sum_i \delta[\mathbf{r}+\mathbf{r}_i(0)-\mathbf{r}_i(t)] \right\rangle$$

(self-correlation) and

$$G_{\mathrm{d}}(\mathbf{r},t) = \frac{1}{N}\left\langle \sum_{i\neq j} \delta[\mathbf{r}+\mathbf{r}_i(0)-\mathbf{r}_j(t)] \right\rangle$$

(distinct correlation). In molecular dynamics these functions are computed directly from the time-dependent atom coordinates.

The self-correlation function compares the position of a particle to its position at later time. In equilibrium this function depends only on the time difference. It produces information about jump and diffusion processes. The distinct correlation compares the position of a particle to the position of an other particle at a different time. It yields information about correlated motions, for instance in a phonon.

From the correlation function several system parameters are derived: the angular averaged distinct correlation function at $t = 0$ is proportional to the radial distribution function $g(r)$, whereas the angular averaged $G_{\mathrm{s}}(\mathbf{r},t)$ reproduces the diffusion profile and thus also the mean square displacement $\langle(\mathbf{r}(t)-\mathbf{r}(0))^2\rangle$.

The form of the van-Hove correlation function is strongly different for solids, liquids, and glasses. In liquids $G_{\mathrm{s}}(\mathbf{r},t)$ has the form of a Gaussian for $t > 0$ and approaches zero with time. $G_{\mathrm{d}}(\mathbf{r},t)$ starts as the radial distribution function and approaches the constant value 1 for large times. On the other hand in solids $G_{\mathrm{s}}(\mathbf{r},t)$ does not decay to zero, but is reduced after a transient time to a constant Gaussian peak with a width determined by temperature. If jump processes occur then satellite peaks are observed in addition to the maximum at $r = 0$. Therefore one may extract from $G_{\mathrm{s}}(\mathbf{r},t)$ directly the elementary diffusion processes and the jump geometry.

In quasicrystals phasonic flips require the possibility of the atoms to occupy alternative places which are less than an interatomic distance apart from the initial point. A pair of such positions is called a split position [25].

The analysis of the van-Hove correlation functions, especially of the self part, provides direct information on flip geometries and flip vectors. To obtain the frequencies and the wave vectors, one has to compute its Fourier transform, the dynamical structure factor.

At first one determines the intermediate scattering function

$$F(\mathbf{k},t) = \frac{1}{N}\int_{V_{\mathrm{sim}}} G(\mathbf{r},t)\exp(\mathrm{i}\mathbf{k}\mathbf{r})\mathrm{d}\mathbf{r}.$$

The dynamical structure factor is then computed from

$$S(\mathbf{k},\omega) = \frac{1}{2\pi}\int_0^{t_{\max}} F(\mathbf{k},t)\exp(\mathrm{i}\omega t)\mathrm{d}t.$$

V_{sim} is the simulation cell, and $t_{\max}$ the simulation time. To obtain a good resolution in $\mathbf{k}$- and ω-domain one should use as many atoms as possible, and the simulations should run as long as possible. Depending on the computational power either the averaged van-Hove correlation function is Fourier-transformed after the simulation or the Fourier-transformed dynamical structure factor is averaged.

Kob [23] has pointed out that effects of the finiteness of the simulation cell play an important role for the dynamical structure factor and that the quality of the structure factor is improved by the second method. It is, however, much more computationally costly, especially on parallel computers.

From the radially averaged dynamical structure function one can compute the static structure factor for $\omega = 0$ which represents the translational order of the structure.

The Van-Hove correlation functions are valuable for geometrical analysis, but the collective behavior of an atom may be derived more easily from the dynamical structure factor. The phonons are given as satellite bands of the static structure factor at $\omega = 0$ with the wave vector $\mathbf{k}$ as a parameter if $S(\mathbf{k}, \omega)$ is represented as a function of ω. The diffusive part is found around $\omega = 0$. For quasicrystals we expect information also about phasons.

The dynamical structure factor often is monitored only as an angular average. This may be justified for isotropic structures. For quasicrystals it is interesting to compute the structure factor separately for their distinguished symmetry directions, especially since direction dependent jump processes [20] have been observed in experiment and should be related to phasonic flip processes.

4 Molecular dynamics

Today molecular dynamics simulations can be carried out for all thermodynamically interesting ensembles. The ordinary Newtonian equations of motion are altered in a proper way to allow for thermostating and constant pressure. The altered dynamics is not a limitation if one is interested in thermodynamical averages only. A time step lasts $\delta t = 0.005$ to 0.01 in dimensionless units, or 10^{-15} s in real time. To compute correlation functions, however, we have to work in the microcanonical ensemble and with the unaltered equations of motions since we are interested in the real paths of the atoms and in the correlations of the real dynamics.

The simulation box of the AlCuCo model contained 3 550 atoms and had the dimension $37.69 \times 32.06 \times 41.06$ Å. We used a portion of the infinite quasicrystal that permitted to introduce periodic boundary conditions. For the icosahedral model we constructed a cubic approximant which contained 2 923 atoms in a box of length 14.4 interatomic distances.

Furthermore one has to use a sample in equilibrium to avoid transients in the correlation functions. We have therefore equilibrated the as-generated structures for a long time with canonical NVT simulations. As a thermostat we used the methods of Brown and Clarke [29] to reduce the initial potential energy to a minimum. It took 2 000 simulation steps at $T = 0.8$ K. Then the samples were equilibrated with the Nosé-Hoover thermostat [30] at $T = 8$ K. The equilibration time was 100 000 steps.

Afterwards the correlation functions were collected at 512 correlation time steps and were averaged over 20 runs at $T = 8$ K also.

4.1 Interactions

For the simulations of the AlCuCo model we have used effective pair potentials which were developed especially for quasicrystals. There are two sets for AlMnSi [31] and AlCuCo quasicrystals [32]. We have tested both sets. First we find that our model is obviously not dynamically optimal: there exist empty decagonal prisms which are filled when the simulation is started. This causes a transient behavior where Al atoms move to the center of the prisms. Second, the Al-potential is very weak at the nearest neighbor distance. Therefore the vibration amplitude of the Al atoms is rather large, and the Al atoms act more or less like a liquid in a solid transition metal frame. The atomic motions caused by these effects are so strong that we have to work at low temperatures. Nevertheless we find that the structure model in general is stable with these potentials. Since the AlMn set works better than the AlCuCo set, we have decided to apply the later ones wince neither set has been adapted especially for our alloy composition.

For the icosahedral model we have applied Lennard-Jones or Dzugutov potentials [33] with parameters tuned to stabilize the shortest atomic distances AA, AB and BB. The results do neither depend qualitatively on the special type of potential nor on the relative depth of the different interactions.

4.2 Correlation functions from molecular dynamics

In liquids and simple crystalline solids all atomic sites are equivalent. One can therefore select one atom or a small number of atoms and compute the correlation functions $G_{\mathrm{s}}(\mathbf{r}, t)$ only for this subset. The computer memory requirements are reduced drastically. For quasicrystals such an approach is not feasible, since one may have of the order of half a hundred different sites which contribute in a different way to the correlation function.

In molecular dynamics the correlation functions can be computed automatically during simulation by collecting histograms as a function of distances and time intervals.

Instead of computing the full space and time-averaged correlation functions $G(\mathbf{r}, t)$ we frequently determined the merely space averaged function $G(\mathbf{r}, \tau)$ where τ is the time from the starting point of the collection of the histogram values. This function yields the jump paths directly, but not the statistical probability.

In practice the computation of correlation functions requires very long simulation runs with a large number of atoms. Nowadays they are performed on massively parallel machines. We have implemented routines for the data collection for correlation functions on vector machines [34] which is rather straightforward due to the shared memory of these machines.

Meanwhile routines for the self-correlation have also been integrated in IMD [35], a program designed for molecular dynamics simulations on massively parallel computers with distributed memory.

On a distributed memory machine the self-correlation function has to be computed first for the atoms on the same processor node and collected for averaging. Second, the correlations for the atoms which have moved from a processing node to its neighbor have to be collected. In a solid where the atoms have a small mobility these two steps should be sufficient. In liquids atoms may have moved to more distant processing nodes, and comparison between more distant nodes are required also.

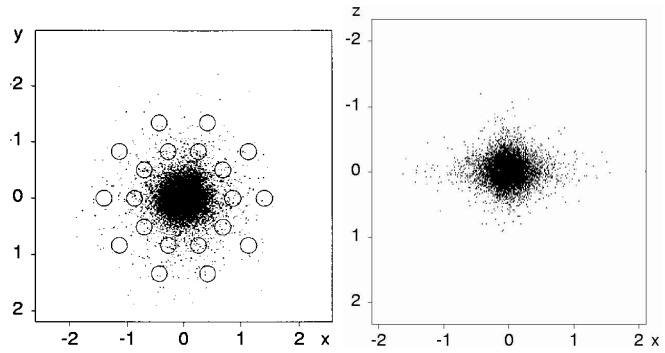

Fig. 5. Self-correlation function $G(\mathbf{r}, t)$ of AlCuCo at a fixed time step. Axis are in Å. Left: quasiperiodic plane. Right: perpendicular plane. The circles indicate the geometrically expected target positions of the flip. The phonon vibrations (central part of the picture) are isotropic, the flips (outer part) are anisotropic.

For the distinct correlation function the situation is more complicated. One may restrict the computation of the distinct correlation function to atoms which are separated only up to a certain distance between the processor nodes. The further approach is similar to the self-correlation function. But if one wants to compute the distinct correlation for any possible distance in a simplistic approach the computational complexity would be quadratic in the number of particles. To avoid such a scaling one can map the torus structure of the simulation box on a ring-like path which touches each processing node once. Then the data have to be moved cyclically from one processing node to a neighbor. This algorithm is linear in the number of particles if the number of atoms per processing node is approximately constant.

5 Results

The self-correlation function has been computed for the decagonal AlCuCo and the icosahedral AlCuLi model.

A restricted decagonal model was used to test the correlation routines. A Tübingen triangle tiling [25] is first transformed into a random tiling by means of Monte Carlo simulations. No energy barriers are taken into account for the flips ($T = \infty$). The initial and final state are then decorated with atoms such as to get AlCuCo samples. If the self-correlation between the two states is computed, an idealized picture is obtained where the thermal fluctuations of the atoms are suppressed. The test has been especially valuable for AlCuCo since the superposition of phonon modes and flips makes an analysis of the atomic motions obtained by molecular dynamics quite complicated.

In the molecular dynamics simulations jumps with the shortest and second shortest distance (resulting from two sequential shortest jumps) could indeed be observed (see Fig. 5). The atoms move to alternative positions which in the first case are less than half an interatomic distance apart from their initial position. Due to this short

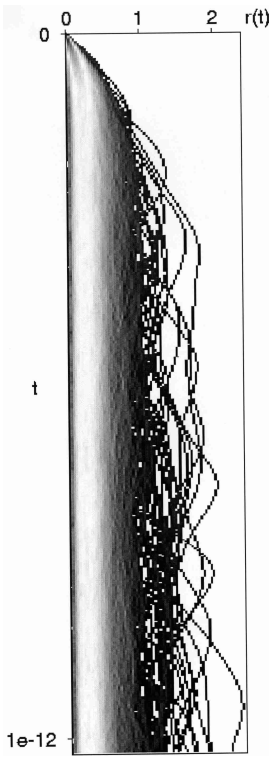

Fig. 6. Self-correlation $G(\mathbf{r}, t)$ of AlCuCo as a density plot of time and distance. The maximum at the left side are the phonon vibrations, whereas flip processes are captured at the right side. The time is given in picoseconds, the distances are in Å.

jump vector the self-correlation could only be computed at low temperatures. Even then the jump processes are partially superposed by phononic vibrations of the atoms around their equilibrium positions. The problem at low temperatures, however, is that only very few jumps occur. If we compare the two plots in Figure 5 we find that the phonon vibrations (the saturated central part of the plots) are three-dimensional isotropic. The jumps (the scattered points at about 0.5 to 1.5 Å) have cylindrical symmetry only. In Figure 5 we also observe that there are preferably in-plane jumps and axial jumps, and only few diagonal jumps, if any.

If one displays the distance of the atoms from their initial position instead of the time-averaged correlation function the paths of the atoms can be studied directly and jumps to alternative positions can be determined unambiguously (Fig. 6). The overwhelming contribution of the phonons to the correlation function can be read from Figure 7. On the right side of the histogram we find again the weak traces of the flips. From these one could in principle derive the frequencies and the jump times of the flips, but for a more detailed and accurate analysis it is better to construct special flip detectors [36,37].

The correlation function $G_s(r, t)$ (Fig. 8) clearly shows a kink at about 0.80 to 0.87 Å. These are the jumps that have been predicted by Zeger from geometrical studies [25]. Then there is a shoulder at 1.4 to 1.45 Å and

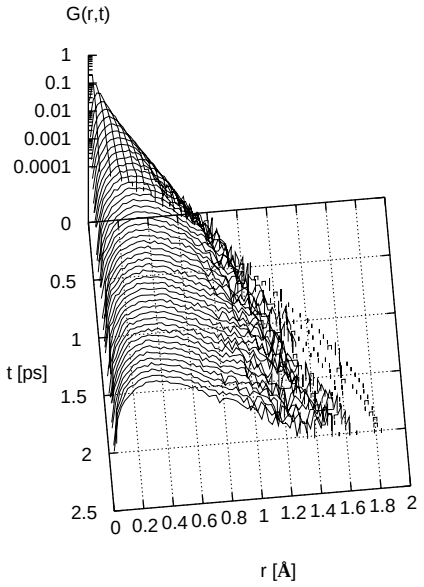

Fig. 7. Self-correlation $G(\mathbf{r}, t)$ of AlCuCo as a histogram of time and distance. The maximum at the left side are the phonon vibrations, whereas flip processes are captured at the right side. The time is given in seconds, the distances are in Å.

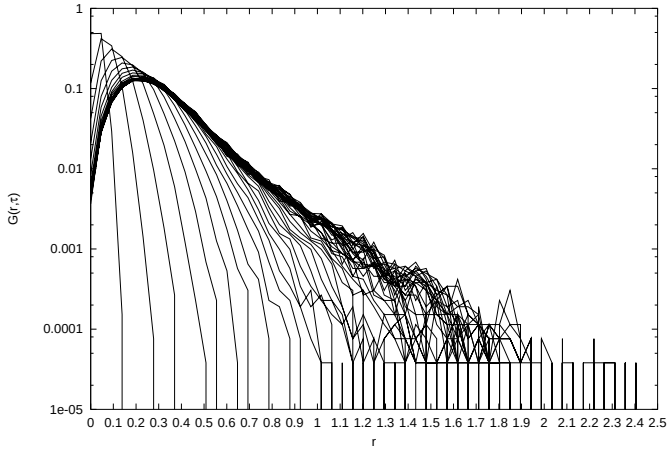

Fig. 8. Angular-averaged self-correlation $G(\mathbf{r}, t)$ of AlCuCo. At the left border one observes phonon vibrations, at the right border flip processes may be seen. The line paths represent different time intervals, with time they move to the right. The distances are in Å.

a maximum at 1.8 Å as well as a weak maximum at 1.6 to 1.65 Å. The shoulder at 1.4 Å can be interpreted as two consecutive jumps of length 0.87 Å with an angle of 72° between them. The maximum at 1.8 Å may be related to the jumps with distance 1.79 Å as predicted by Zeger.

The self-correlation has also been computed for the icosahedral AlCuLi model [38]. No flips are observed, only nearest neighbor jumps occur. Therefore the problem of superposition with phonon vibrations does not show up. If the self-correlation function is plotted at constant time intervals we obtain a series of decreasing maxima at separations which are close to the nearest neighbor distance. The interpretation is that atoms jump successively from one atom site to the next. Furthermore, if the temperature is lower than 60% of the melting temperature, only A atoms move, whereas B atoms only vibrate. This picture changes completely at higher temperatures: the jumps of A atoms are replaced by long-range diffusion where all atoms at all sites take part equally.

Details for this model and for modifications thereof have been recorded elsewhere [38].

6 Discussion

Apart from the icosahedral model there exists a geometrically rather similar monatomic dodecagonal model [39] related to the NiCr quasicrystal structures. The results for this model are, however, drastically different from the icosahedral case: the atoms are jumping in one-dimensional chains parallel to the periodic direction. Triggered by these jumps are rearrangements of the tiling. An important difference between the two models is the monatomic nature of the dodecagonal structure which simplifies the interchange of atoms. In the icosahedral model even geometrical flips are rather hard to find. First steps have been taken to solve this problem [40]. A new tile, a twin of two rhombic dodecahedra has to be introduced to enable flips in the binary version of the icosahedral model. No molecular dynamics simulations have been carried out yet for this variant.

The decagonal model on the other hand is structurally quite different from the dodecagonal model with respect to topological atom arrangement and packing density. The flips are, however, rather similar (the icosahedral and dodecagonal model are densely packed Frank-Kasper-phases, the dodecagonal model is not densely packed). The decagonal and the dodecagonal model are both layered in contrast to the icosahedral model. Similar motions of atoms are permitted in all layers, and flips of tiles are observed. But the similarities end here already: in the dodecagonal the atoms move long distances along the periodic direction whereas they are almost completely confined to the layers in the decagonal model.

In conclusion we find that the atomic motion, *i.e.* flips or jumps of the atoms depend strongly on the quasicrystal type. No general rules can be determined up to now.

We have demonstrated that correlation functions of quasicrystals can be computed successfully directly by molecular dynamics simulations. The computations are, however, very time-consuming (this has been expected). The interpretation of the results is further complicated by the fact that we have a discrete structure, but atomic jumps which connect sites closer than the nearest neighbor distance. Such jumps do not even occur in glasses, and therefore the study of disordered glasses is easier with respect to atomic jumps.

We have implemented programs that allow us to compute different types of correlation functions. First results have been reported and compared to other results obtained by direct observation of the jumps and flips with flip detectors. Further extensive molecular dynamics

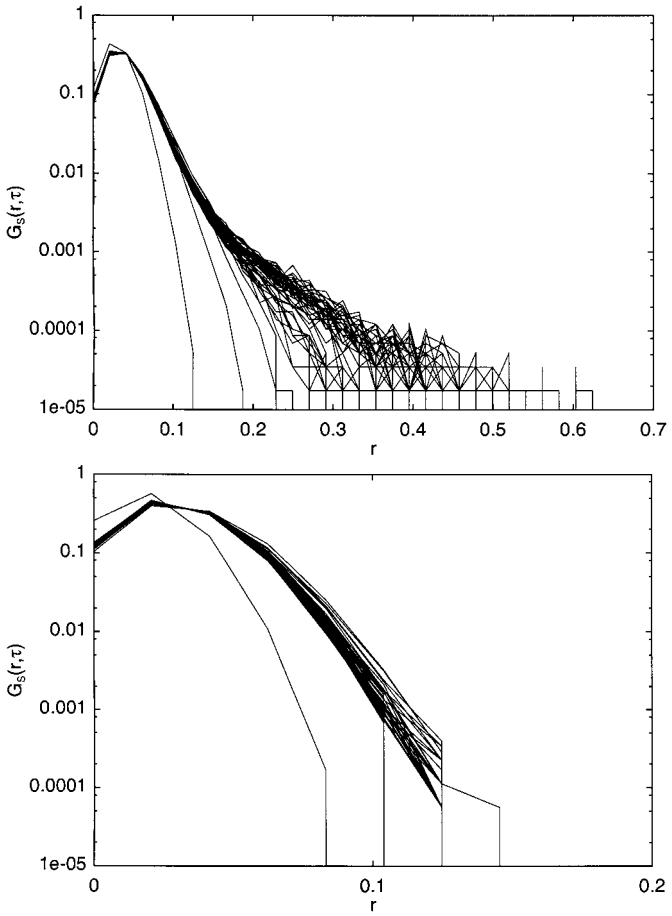

Fig. 9. Histogram of the atom jumps at low temperatures. Radius is given in interatomic distances. Top: A atoms. Bottom: B atoms. The different line paths represent different time intervals, with time they move to the right. A comparison of the two pictures shows that only A atoms jump whereas the B atoms only vibrate. The jump rates are 33 jumps per 10 000 atoms and 10^5 time steps at $T = 0.55T_{\mathrm{melt}}$, the jump times are of the order of the vibration period.

simulations are required to collect more data. An interesting application is the study of the collective motion of the atoms which can hardly be captured by direct observation of single jumping atoms.

The authors are indebted to their colleagues at the Institut für Theoretische und Angewandte Physik for helpful discussions, especially to Gabriele Zeger.

References

1. P. Bak, Phys. Rev. B **32**, 5764 (1985).
2. T.C. Lubensky, S. Ramaswamy, J. Toner, Phys. Rev. B **32**, 7444 (1985).
3. A.I. Goldman, C. Stassis, M. de Boissieu, R. Currat, C. Janot, R. Bellissent, H. Modden, F.W. Gayle, Phys. Rev. B **45**, 10280 (1992).
4. M. Windisch, J. Hafner, M. Krajčí, M. Mihalcovič, Phys. Rev. B **49**, 8701 (1994).
5. M. de Boissieu, M. Boudard, R. Bellissent, M. Quichilini, B. Hennion, R. Currat, A.I. Goldman, C. Janot, J. Phys. Cond. Matt. **5**, 4945 (1993).
6. M. Boudard, M. de Boissieu, S. Kycia, A.I. Goldman, B. Hennion, R. Bellisent, M. Quichilini, R. Currat, C. Janot, J. Phys. Cond. Matt. **7**, 7299 (1995).
7. J.-B. Suck, J. Non-Cryst. Sol. **158–159**, 872 (1993).
8. C.L. Henley, V. Elser, Phil. Mag. B **53**, L59 (1986).
9. S.E. Burkov, Phys. Rev. B **47**, 12325 (1993).
10. J. Hafner, M. Krajčí, J. Phys. Cond Matt. **5**, 2489 (1993).
11. J. Hafner, M. Krajčí, M. Mihalcovič, Phys. Rev. Lett. **76**, 2738 (1996); 31 (1993); Phys. Rev. B **47**, 1084 (1993).
12. J. Los, T. Janssen, F. Gähler, J. Non-Cryst. Sol. **153 & 154**, 581 (1993).
13. G. Kasner, H. Böttger, Int. J. Mod. Phys. B **7**, 1487 (1993).
14. G. Poussigue, C. Benoit, A. Azougarh, M. de Boissieu, R. Currat, J. Phys. Cond. Matt. **6**, 659 (1994).
15. E. Cockayne, M. Widom, Phil. Mag. A **77**, 593 (1998).
16. P. Kalugin, A. Katz, Europhys. Lett. **21**, 921 (1993).
17. M.V. Jarić, E.S. Sørensen, Phys. Rev. Lett. **73**, 2464 (1994).
18. G. Coddens, C. Soustelle, R. Bellissent, Y. Calvayrac, Europhys. Lett. **23**, 33 (1993).
19. G. Coddens, S. Lyonnard, Physica B **226**, 28 (1996).
20. G. Coddens, Abstract, Krakow (1996).
21. Th. Zumkley, H. Mehrer, K. Freitag, M. Wollgarten, N. Tamura, K. Urban, Phys. Rev. B **54**, R6815 (1996).
22. R. Blüher, P. Scharwaechter, W. Frank, Phys. Rev. Lett. **80**, 1014 (1998).
23. W. Kob, H.C. Andersen, Phys. Rev. E **51**, 4626 (1995); E **52**, 4134 (1995).
24. H. Teichler, *Simulationstechniken in der Materialwissenschaft*, Freiburger Forschungshefte B **279**, (Technische Universität Bergakademie Freiberg, 1996), p. 215.
25. G. Zeger, H.-R. Trebin, Phys. Rev. B **54**, R720 (1996).
26. G. Zeger, Diplomarbeit, Stuttgart, 1995.
27. W. Steurer, personal communication, 1994.
28. J. Roth, R. Schilling, H.-R. Trebin, Phys. Rev. B **41**, 2735 (1990).
29. D. Brown, J.H.R. Clarke, Mol. Phys. **51**, 1243 (1984).
30. W.G. Hoover, Phys. Rev. A **31**, 1695 (1985).
31. J. Zou, A.E. Carlsson, Phys. Rev. Lett. **70**, 3748 (1993).
32. R. Phillips, J. Zou, A.E. Carlsson, M. Widom, Phys Rev. B **49**, 9322 (1994).
33. M. Dzugutov, Phys. Rev. Lett. **70**, 2924 (1993).
34. M. Hohl, Diplomarbeit, Stuttgart, 1997.
35. J. Stadler, R. Mikulla, H.-R. Trebin, Int. J. Mod. Phys. C **8**, 1131 (1997), `www.itap.physik.uni-stuttgart.de/~imd/index.html`.
36. D. Wolfangel, diploma thesis, Stuttgart, 1998.
37. D. Bunz, diploma thesis, Stuttgart (1999); D. Bunz, G. Zeger, J. Roth, M. Hohl, H.-R. Trebin, Proc. of the ICQ7, Stuttgart, 1999.
38. J. Roth, Euro. Phys. J. B **15**, 7 (2000).
39. J. Roth, F. Gähler, Euro. Phys. J. B **6**, 425 (1998).
40. C. Rudhart, Staatsexamensarbeit, Stuttgart, 1999.